



One pot and green ultrasonic catalytic synthesis of catenated nanocellulose by sodium 30-tungston pentaphosphate polyoxometalate as an interlocked surface stabilizer and its application for surface loading of L-ascorbic acid

Sara Saneinezhad¹ · Fatemeh F. Bamoharram¹ · Mehdi Pordel¹ · Javad Baharara²

Received: 1 January 2020 / Accepted: 25 July 2020 / Published online: 18 August 2020
© Institute of Chemistry, Slovak Academy of Sciences 2020

Abstract

Among different biopolymers, cellulose being the first abundant biopolymers in nature has many fascinating properties, including low cost, good biodegradability, and excellent biocompatibility, which made cellulose a real potential material to create nano-drug delivery systems. Regarding, emphasis of science and technology shifts toward environmentally friendly and sustainable resources and processes, herein, we report a facile, one pot and green synthesis of the catenated assemblies of cellulose nanoparticles (CNPs) via acidic catalysis in the presence of preyssler heteropolyacid. This fast, green, and high-yield catalytic synthesis reduces the time of reaction to 15 min using low-intensity ultrasonic waves of 150 W. CNPs were characterized by transmission electron microscopy, scanning electron microscopy, particle size distribution analysis, Fourier-transformed infrared spectroscopy, X-ray diffraction, and atomic force microscopy. The results showed that catenated CNPs exhibit spherical-like structures with widths and lengths of 35–40 and 50–150 nm, respectively. The CNPs showed a surface charge of -35.2 mV, which allows obtaining a stable colloidal suspension. Moreover, cellulose nanoparticles loaded with ascorbic acid (CNPs/AA) were engineered and ascorbic acid could be released from the CNPs/AA in a controlled manner for 1 h.

Keywords Ultrasonic synthesis · Catenated cellulose · Preyssler · Heteropolyacid · Ascorbic acid · Nanoparticles

Electronic supplementary material The online version of this article (<https://doi.org/10.1007/s11696-020-01296-x>) contains supplementary material, which is available to authorized users.

✉ Fatemeh F. Bamoharram
abamoharram@yahoo.com; fbamoarram@mshdiau.ac.ir

Sara Saneinezhad
saneinezhad@yahoo.com

Mehdi Pordel
mehdipordel58@yahoo.com

Javad Baharara
baharara@yahoo.com

¹ Department of Chemistry, Mashhad Branch, Islamic Azad University, Mashhad, Iran

² Department of Biology, Mashhad Branch, Islamic Azad University, Mashhad, Iran

Introduction

Over the past few decades due to their unique and valuable properties, nanostructures as nanocarriers with various shapes and sizes have been fabricated (Chamundeeswari et al. 2019) and large variety of them have been used in the delivery of various drugs, including peptides, proteins, and nucleic acids (Kingsley et al. 2006; Mishra et al. 2010; Sun et al. 2014; How et al. 2013; Lopez-Davila and Loizidou 2012; Bhatia 2016; Malam et al. 2009; Muller 2000; Levi-Polyachenko et al. 2009; Madani et al. 2011; Yavuz et al. 2009; Loo et al. 2005; Kim et al. 2008; Hallan et al. 2014; Geibler et al. 2010; Freeman et al. 2011; Qian et al. 2012; Yoo et al. 2005).

Additionally, in the field of biotechnology, biopolymers have been extensively investigated for various drug delivery applications and through in vitro and in vivo studies have affirmed their potential as drug carriers (Jacob et al. 2018). The major reason that biopolymers have

gained popularity as carriers for drug delivery is that they offer a plethora of advantages over conventional polymers. Biopolymers are non-toxic and biocompatible, thus making them a versatile carrier. They offer the economic advantage, as they are relatively cheap and offer environmental advantages as well because they are biodegradable (Singh 2011).

Polysaccharides are the new trends in nanomaterial-based drug delivery systems mainly using biopolymers such as proteins (silk fibroin, collagen, gelatin, and albumin), chitosan, alginate, cellulose, and starch (Jacob et al. 2018; Pathania et al. 2016). Another emerging class of biopolymers is peptide- and polypeptide-based polymers which have arisen due to the amalgamation of protein engineering and macromolecular self-assembly (Goudoulas 2012).

Among different biopolymers, cellulose being the first abundant biopolymers in nature has many fascinating properties, including low cost, good biodegradability, and excellent biocompatibility, which made cellulose a real potential material to create nano-drug delivery systems (Kim et al. 2013). The reason for using cellulose and its derivatives as drug excipients is that they are porous materials, which can facilitate the liquid uptake. Cellulose can interact strongly with water, thus swelling readily in water (Lee et al. 2014). It is well known that a fast swelling drug will have a quick dissolution process. In these applications, cellulose and its derivatives generally can modify the solubility/gelling behavior of drugs, resulting in different mechanisms for controlling the release profiles of drugs. Therefore, the drug delivery systems with cellulose and its derivatives as excipients can have both immediate and sustained delivery of drugs without compromising the therapeutic performance.

Nanocellulose has generated a high interest as drug carrier, because of its properties including large surface to volume ratio, high tensile strength and stiffness, high flexibility, and good electrical and thermal properties (Deepa et al. 2011). Sulfuric acid is the most common acid for nanocellulose preparation through chemical hydrolysis (Börjesson and Westman 2015) but it is possible to use other acids as well. Hydrochloric acid, hydrobromic acid, and phosphoric acid have been used for nanocellulose preparation but compared to sulfuric acid, hydrochloric acid, and hydrobromic acid will not have any surface charges and a stable colloidal dispersion is, therefore, harder to form. Phosphoric acid will give charged phosphate groups on the nanocrystal surface. Among the various types of catalysts, ionic liquids, which are composed of both cations and anions, are particularly promising (Bee Abd Hamid et al. 2014). Enzymatic hydrolysis using celluloses, (Henriksson et al. 2007; Siqueira et al. 2010) and TEMPO (2,2,6,6-tetramethylpiperidin-1-oxyl)-mediated oxidation, (Saito et al. 2007) have also been reported to prepare cellulosic nanoparticles (Man et al. 2011) Recently, a new method using a gas-phase

hydrochloric acid hydrolysis at room temperature for 30 min was patented (Kontturi et al. 2011).

Among these methods, acid hydrolysis method (Purkait et al. 2011) is the earliest and well-rounded method for preparing nanocellulose, but the later waste liquid recovery is difficult. The enzymatic hydrolysis method (Satyamurthy et al. 2011; Zhu et al. 2011) is non-polluting, but the efficiency is low. So, more and more researchers are committed to developing more efficient and environmentally friendly catalytic methods (Deepa et al. 2011; Kaushik and Singh 2011).

Heteropoly acids (HPAs) are well-defined solid acids that are remarkable for their molecular and electronic structural diversity and their significance is quite diverse in acidic catalysis (Khadempir et al. 2016; Saneinezhad et al. 2019). Preyssler as a solid acid introduced as promising candidates for green catalysts. It is green with respect to corrosiveness, safety, quantity of waste, and separability and with 14 acidic protons, is an efficient “super acid” solid catalyst which can be used in different reactions instead of sulfuric acid (Bamoharram et al. 2006, 2013; Ayati et al. 2014).

Concerning the great success of preyssler for green catalysis and our interest in developing the preyssler application, this study deals with the facile synthesis of catenated nanocellulose with the help of preyssler catalyst. We have also investigated the application of the catenated nanocellulose obtained as a carrier of ascorbic acid for further studies.

The novelty of this paper is not only the high-yield formation of nanocellulose in catenated form, but also is the use of green and eco-friendly preyssler catalyst, as an interlocking surface stabilizer and linker to interfacial adhesion of cellulose nanoparticles through hydrogen bonds locking. In comparison to other methods, the main advantages are the synthesis involved (1) aqueous phase, (2) using green and an eco-friendly solid acid catalyst, (3) high yield, (4) no waste, (5) easy recovery of the catalyst and (6) safety, so it could be termed as green nanotechnology for drug and vitamin delivery applications.

Materials and methods

Materials

Microcrystalline cellulose (cotton linters powder, purity 100%) was purchased from Sigma-Aldrich and was used as received. $H_{14} [NaP_5W_{30}O_{110}]$ was prepared using sodium tungstate dihydrate (purity > 99%) and orthophosphoric acid (purity 85%) according to our earlier works as below (Bamoharram et al. 2006). Preyssler acid was prepared by the passage of a solution of potassium salt in water through a column of Dowex 50WX 8 in the H^+ form and evaporation of the elute to dryness under vacuum. L-ascorbic acid

(purity > 99%) was purchased from Sigma-Aldrich. Distilled water was used throughout the experiment.

Synthesis of catenated cellulose nanoparticles (CNPs)

The microcrystalline cellulose was suspended in deionized water at 2:20 (w/v) and was sonicated at room temperature in the presence of preyssler heteropolyacid (8% w/w) using a 150 W power output ultrasonicator probe. Ultrasonic treatment was conducted at room temperature and 15 min. The suspension was obtained by extraction of diethyl ether and dried in an oven (50–60 °C), while the white powder was stored in a vacuum desiccator.

Synthesis of cellulose nanocrystal-ascorbic acid complex

Ascorbic acid (AA) was added to CNPs suspension (2 g of CNPs in 5 mL distilled water). The obtained suspension has been shaken by a shaker at room temperature for 45 min. After that, the suspension containing ascorbic acid/CNPs was centrifuged at 6000 rpm for 20 min to settle down the complex. The supernatant was collected, and then, the concentration of unbound AA was determined using a UV–visible spectrometer at 264 nm. The concentration of bounded AA in the CNPs/AA was calculated according to the following formula: bounded AA = [added AA] – [unbounded AA].

Characterization

Scanning electron microscopy (SEM) (VEGA\\TESCAN-XMU, Czech Republic), energy-dispersive spectrometry (EDS) (Mira 3-XMU, Czech Republic), Zetasizer (ZS) (Malvern, UK), Transmission electron microscopy (TEM) (Hitachi HT7700 instrument), Fourier transform infrared spectroscopy (FTIR) (Avatar.370 FTIR Thermo Nicolet spectrophotometer, England), Atomic force microscopy (JPK-NanoWizard II, Germany) and UV–visible spectrophotometer (Optizen UV3220, Germany) were used for analyzing the materials.

In vitro ascorbic acid release procedure

The prepared CNPs/AA complex was suspended in 1 mL distilled water and transferred to a dialysis tube. At room temperature, the dialysis tube was placed in the releasing media (water), which was kept for 240 min under mild stirring. An aliquot (1 mL) of the releasing media was removed at predetermined time intervals and its absorbance was measured using a UV–vis spectrometer at a wavelength of 264 nm. One mL of release medium was sampled every 10 min and replaced by a fresh medium. The absorbance

data are converted to concentration using a calibration curve, previously built using standard AA concentrations.

Results and discussion

Catalytic ultrasonication

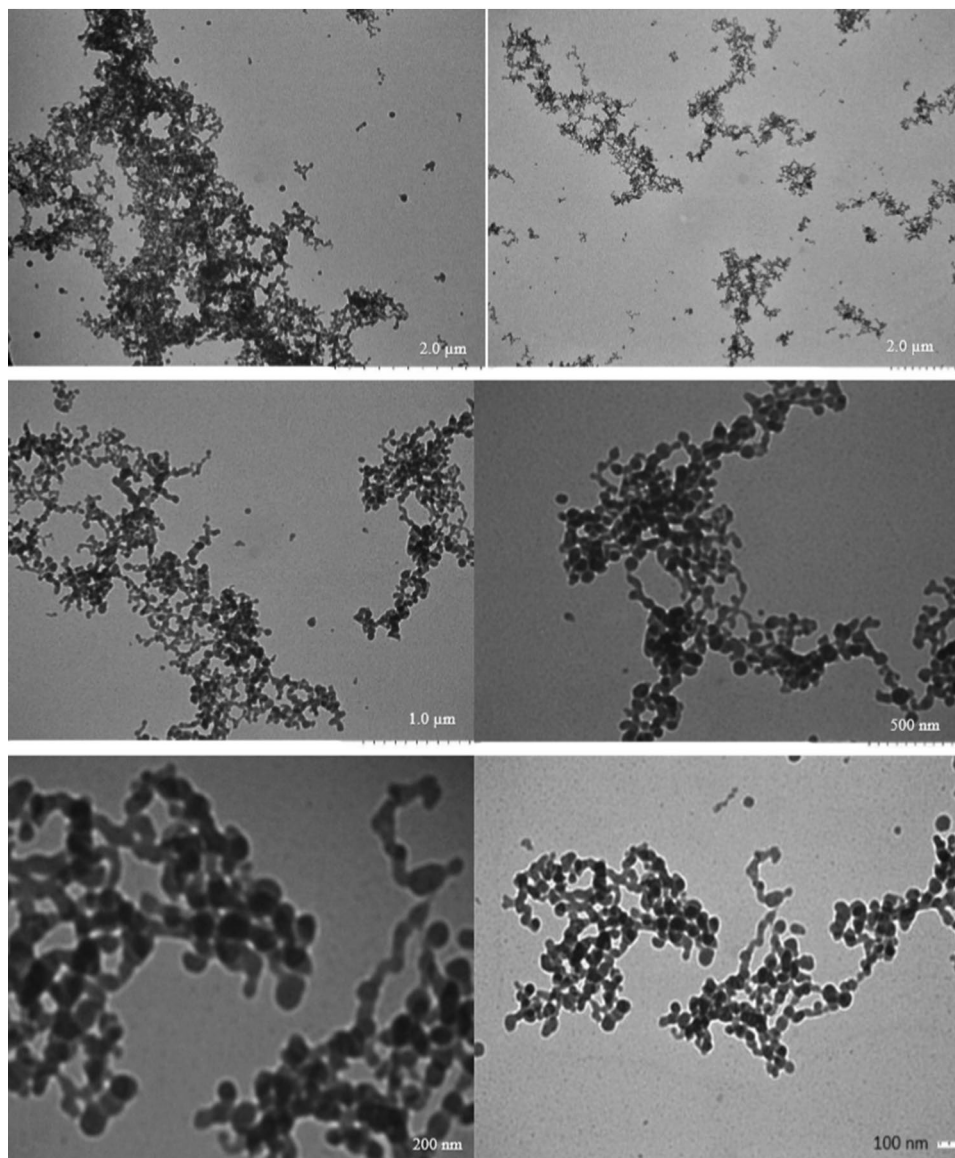
The catalytic sonication technique is industrially feasible because the process has a low impact on the environment (Liu et al. 2014). The synthesis of CNPs was performed with a one-pot synthesis technique in the presence of preyssler heteropolyacid. The used method is simple and efficient and takes place within a short time at ambient temperature. The highest yield of CNPs (100%) was achieved when cellulose and preyssler catalysts are exposed to the sono-mechanical treatment under sonication power and time reaction 150 W and 15 min, respectively.

It is known that ultrasonic treatment may swell and open the cellulose fibers, enhancing the possibility of acid attack (Li et al. 2012). Therefore, it is possible potentially to decrease the hydrolysis reaction time using an ultrasonication process in the presence of acidic catalyst. In support of this suggestion, Keggin type heteropolyacid under hydrothermal condition (i.e., at higher reaction temperatures than 100 °C) did not produce nanocellulose (Tian et al. 2010). As an acid catalyst, Preyssler helps to increase the rate of hydrolysis of cellulose to nanocellulose under sonochemical conditions as compared with the absence of preyssler. A large amount of energy could be released in the presence of the ultrasonic waves which led to the disruption of cellulose's hydrogen bonding network. Hence the breaking of the strong glycosidic bonds of the crystalline portion of cellulose, which together with the breaking of the interconnected hydrogen bond network, causes the structure to open. It suggests that the ultrasonic power could speed up the accessibility of the preyssler catalyst into the cellulose's internal spaces, because the energy and pressure gained during the process loosen the cellulose's compactness. This is in line with previous researches (Bee Abd Hamid et al. 2016).

Transmission electron microscopy

To obtain the size and morphology of the synthesized CNPs, they were characterized by TEM. TEM images of catenated cellulose nanoparticles in the presence of Preyssler HPA with different magnifications (100 nm–2 μ) have been shown in Fig. 1. This figure shows that the catenated assemblies of cellulose nanoparticles (CNPs) have been formed by preyssler as a linker which is due to interfacial adhesion through hydrogen bonds locking. It is attributed to the stabilizing role of the preyssler and hydrogen bond formation in the secondary structure of the heteropolyacid, respectively.

Fig. 1 TEM images of catenated cellulose nanoparticles in the presence of Preyssler HPA with different magnifications



Generally, solid HPAs form ionic crystals composed of heteropolyanions, counteranions, and hydration water. Preyssler units with phosphorus as the central atom and 30 tungsten atoms have a charge of 14 and to balance the negative charge on the preyssler anion, 14 protons are needed (Misono 1987). The overall composition is then $H_{14}[NaP_5W_{30}O_{110}]$. Additionally, preyssler anion has three types of oxygen atoms as potential protonation centers: terminal oxygens $M=O$ and two types of bridging oxygens $M-O-M$, edge sharing, and corner sharing (Fig. 2). In solid HPAs, the protons take part in the formation of the HPA crystal structure, linking the neighboring heteropolyanions. In this case, the more accessible terminal oxygens can be protonated. Heteropolyacids have primary and secondary structures that determine the secondary structure by the number of hydration waters found in the solid (Okuhara

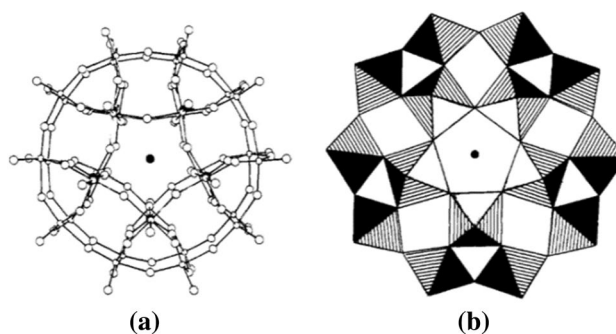


Fig. 2 Preyssler structure, (a) an ORTEP view looking approximately along the virtual C_s symmetry axis and (b) an idealized view along C_s showing the WO_6 octahedra in the upper half of the anion (Alizadeh et al. 1985)

et al. 1996). In a hydrated sample, hydrogen bonds help preserve the secondary structure. In the hydrated form, the protons that sit between the water molecules in the center of the secondary cavity, thus forming a species of $H_5O_2^+$ (Kozhevnikov 1987). Each proton site in preyssler links four neighboring heteropolyanions by forming hydrogen bonds with the terminal $W=O$ oxygens and lead to the formation of the catenated structure of nanocellulose (Fig. 3).

All of the TEM images support the presence of preyssler as stabilizer around the CNPs (brighter circles) and confirm that the catenated CNPs have diameters ranging from 35 to 40 nm. The length of nanocellulose was observed hundreds of nanometers similar to earlier

observations (Liu et al. 2014). The existence of the negatively charged preyssler on the CNPs surface as a stabilizer causes the formation of an electrostatic layer around the CNPs and leads to the dispersion in water as well as preventing flocculation and sedimentation.

Size distribution curve

Figure 4 plotted the size distribution curve from the TEM picture. The average distribution curve size was 36.83 ± 5 nm, well in line with the TEM picture (38 ± 8 nm).

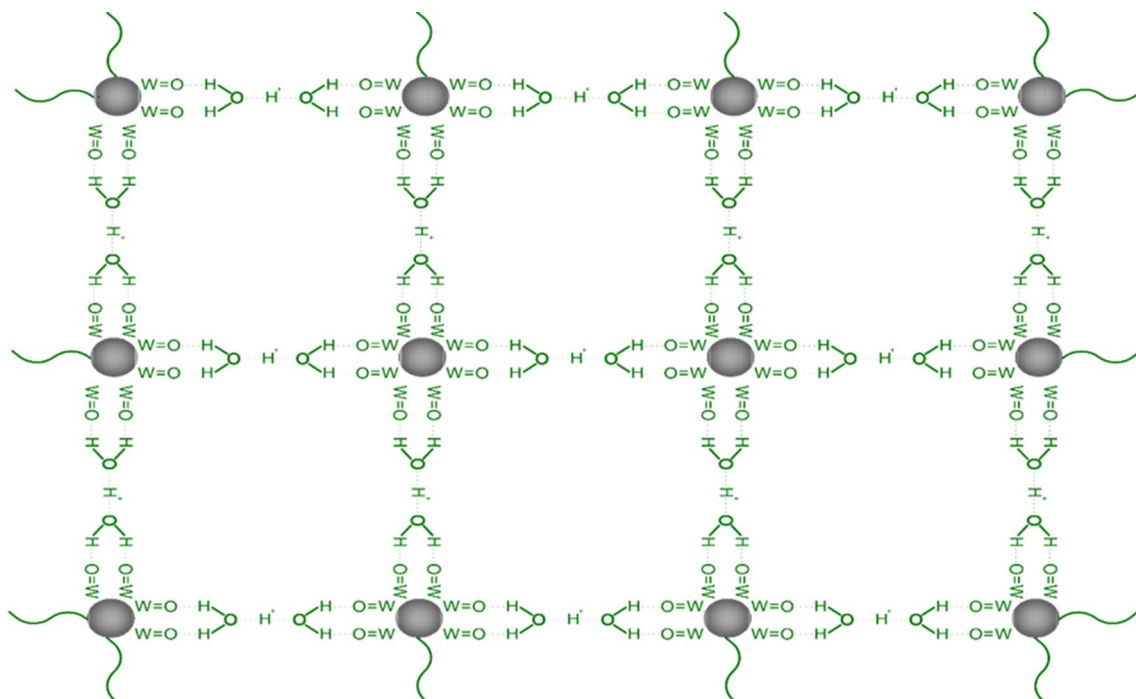
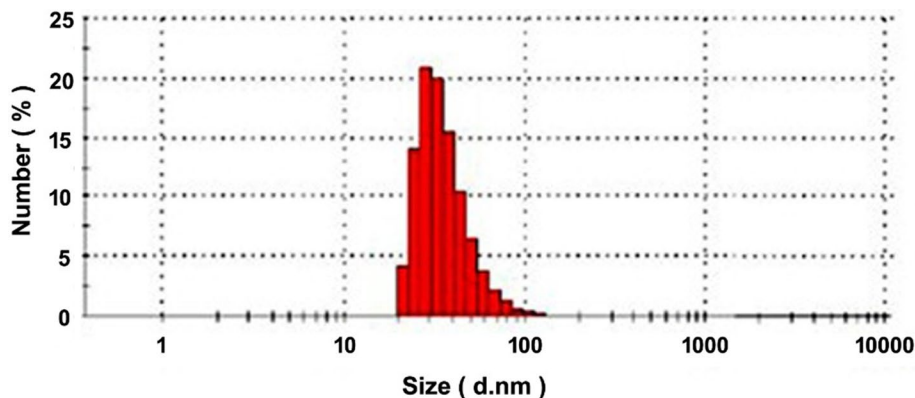


Fig. 3 The catenation of cellulose nanoparticles by preyssler HPA via hydrogen bonding, where the gray balls are the MCC units which surrounded by tungsten atoms of preyssler acid through terminal $W=O$

bonds. The units are connected to each other through hydrogen bonding with water molecules

Fig. 4 The size distribution curve of catenated cellulose nanoparticles



Atomic force microscopy (AFM)

Atomic force microscopy is a powerful technique that can provide the direct spatial mapping of surface morphology with nanometer resolution and allows for the study of morphological characteristics of samples (Gu et al. 2005). Figure 5a shows the AFM image of the CNPs locking by preyssler with the spherical shape. A topographical map of CNPs is presented in Fig. 5b in which the highlighted regions indicate rough surface morphology with dents and irregularities. Such rough surfaces have more active sites, offering a greater number of catalytic reaction contact points (Chaudhari et al. 2005, Lee and Lee 1997). Figure 5a shows the catenated structures of cellulose which is well following the TEM image. It is suggested that considerable adhesion/locking between CNPs mediated by the preyssler resulted in the self-assembly of particles towards catenated structures.

Figure 6 shows AFM topography images of CNPs/AA. It can be seen that the AA-coated cellulose nanoparticles show

that the surface is mostly covered by spherical structures which are in turn composed of AA aggregates.

Zeta potential measurement

Colloidal dispersions are subject to several kinds of instability. The particles can stick to each other (aggregation, coagulation, and flocculation), they can stick to surrounding surfaces (deposition) and they can separate under gravity (sedimentation or creaming). These mechanisms all can be counteracted by strong electrostatic repulsion, and the strength of that repulsion can be parameterized by the zeta potential. Strong electrostatic repulsion can prevent aggregation by keeping colloidal particles well separated from each other and from surfaces. To be effective, the electrostatic repulsion should be substantially larger than the thermal energy scale at length scales where van der Waals attraction and other molecular-scale attractions could become dominant. This means that the range of the electrostatic

Fig. 5 AFM images of catenated nanocellulose (a) typical medium scale AFM image ($30 \times 30 \mu\text{m}$), (b) topographical map of the catenated nanocellulose

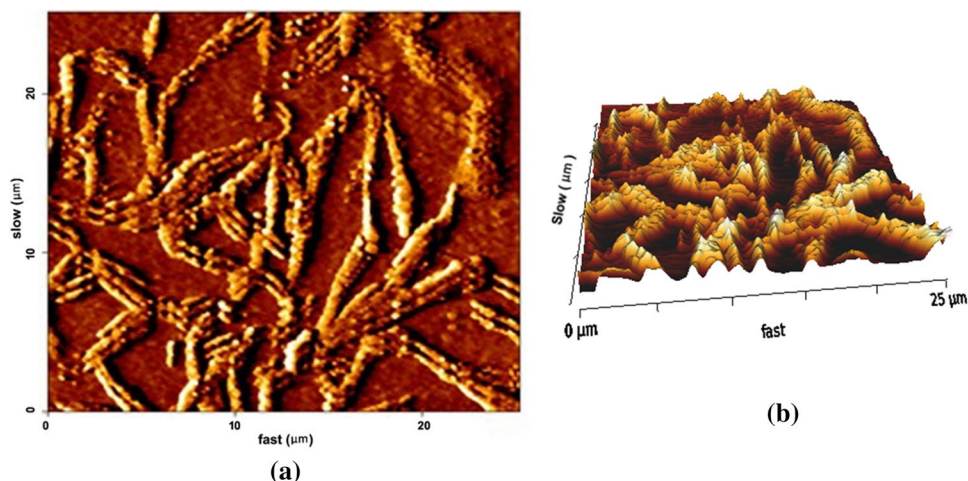
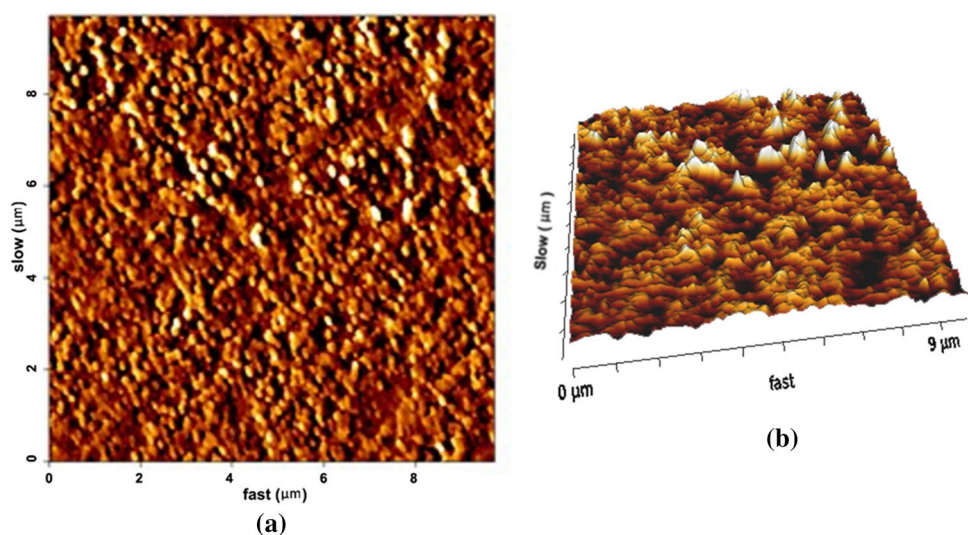


Fig. 6 AFM images of the catenated nanocellulose/ascorbic acid (a) typical medium scale AFM image ($9 \times 9 \mu\text{m}$), (b) topographical map of the catenated nanocellulose/ascorbic acid



interaction must be long enough, and typically means that the ionic strength must be low. In conclusion, the zeta potential is a key indicator of the stability of colloidal dispersions and the magnitude of the zeta potential indicates the degree of electrostatic repulsion between adjacent, similarly charged particles in a dispersion.

As observed from zeta potential data reported in Fig. 7, the breaking of hydrogen bonds significantly impacts the surface charge of CNPs. According to the literature, a value between 0 and 15 mV shows the beginning of nanocellulose agglomeration, sedimentation and flocculation (Zhou et al. 2012), while higher or lower values than 30 mV are generally considered to increase enough mutual repulsion to provide good stability to the colloidal suspension. The results recorded in Fig. 7 show the CNPs display a surface charge of -29.6 mV, which allows a stable colloidal suspension to be obtained. This is due to the negatively charged preyssler heteropolyacids acting as a stabilizer on the surface of the CNPs, which encourages the formation of an electrostatic layer covering the CNPs and the water dispersion, thereby preventing it from flocculating and sedimenting.

Fourier transform infrared spectroscopy

Figure 8a shows the FT-IR spectra of the microcrystalline cellulose. A strong band at ~ 3500 cm^{-1} , is related to the stretching vibration of O–H groups. The characteristic peak around 2800 cm^{-1} is attributed to the symmetric C–H vibrations. An adsorption band around 1700 cm^{-1} is due to the absorbed water. Additionally, the peaks at around 1200, and

670 cm^{-1} are related to the stretching vibration intermolecular ester bonding, and C–OH out-of-plane bending mode, respectively. Maintaining of the cellulose peaks in Fig. 8a indicates that CNPs could maintain the typical structure in cellulose.

The existence of the preyssler on the surface of the synthesized CNPs was confirmed by the FTIR spectroscopy since the peaks correspond to the preyssler, present in the solution in the FTIR spectrum of the stabilized CNPs (Fig. 8c). The composition of Preyssler gives rise to four oxygen forms that are responsible for the preyssler anion fingerprint bands between 1200 and 600 cm^{-1} . The Preyssler structure's characteristic bands $[\text{NaP}_5\text{W}_{30}\text{O}_{110}]^{14-}$ are three bands due to P–O stretching at ~ 1163 cm^{-1} , 1079 cm^{-1} , and 1022 cm^{-1} , two bands attributed to W–O–W at 940 cm^{-1} and 915 cm^{-1} , a band at 750 cm^{-1} corresponding to W=O and a band at 536 cm^{-1} due to P–O bending (Fig. 8b). Compared to Fig. 8a and the initial Preyssler structure (Fig. 8b), in Fig. 8c, there are the bands that emerge from the catenated CNPs and Preyssler.

The IR bands of the CNPs, AA, and CNPs/AA are given in Fig. 9. For ascorbic acid in Fig. 9b, the strong absorption at 1753 cm^{-1} has been attributed to the C=O stretching of the five-membered lactone ring system along with the intense band at 1668 cm^{-1} arising from C=C stretching vibrations. Different vibrational bands are observed in the area 1200 – 1500 cm^{-1} assigned to the modes of scissoring, twisting and wagging of CH_2 , and deformation of C–H. CH_2 scissoring is attributed especially to the weak bands at 1463 cm^{-1} . The band at ~ 1277 cm^{-1} originates

Fig. 7 Zeta potential curve of the catenated nanocellulose

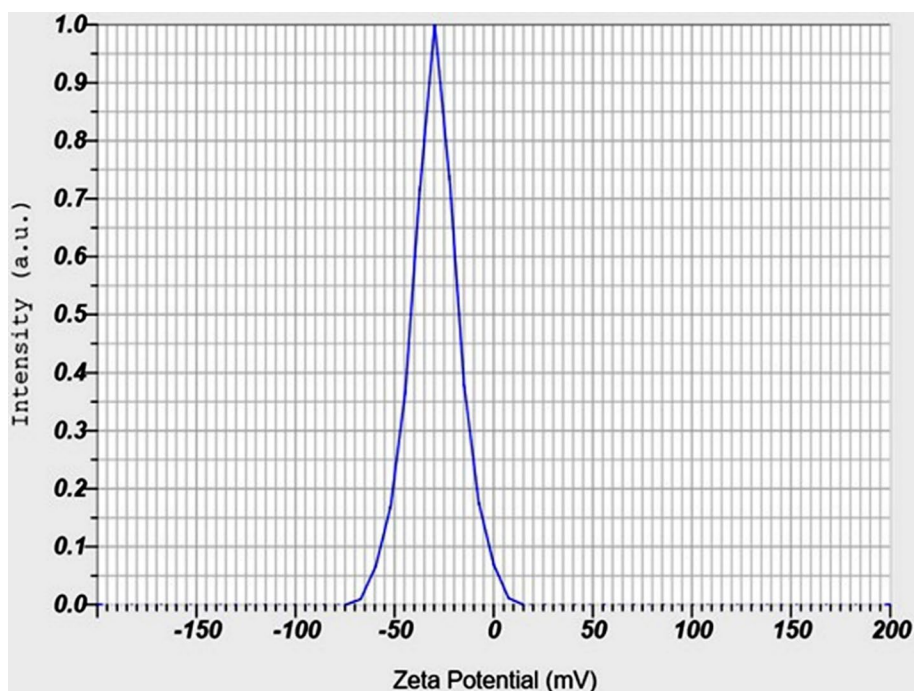


Fig. 8 FTIR spectra of (a) cellulose, (b) Preyssler acid, and (c) catenated preyssler cellulose

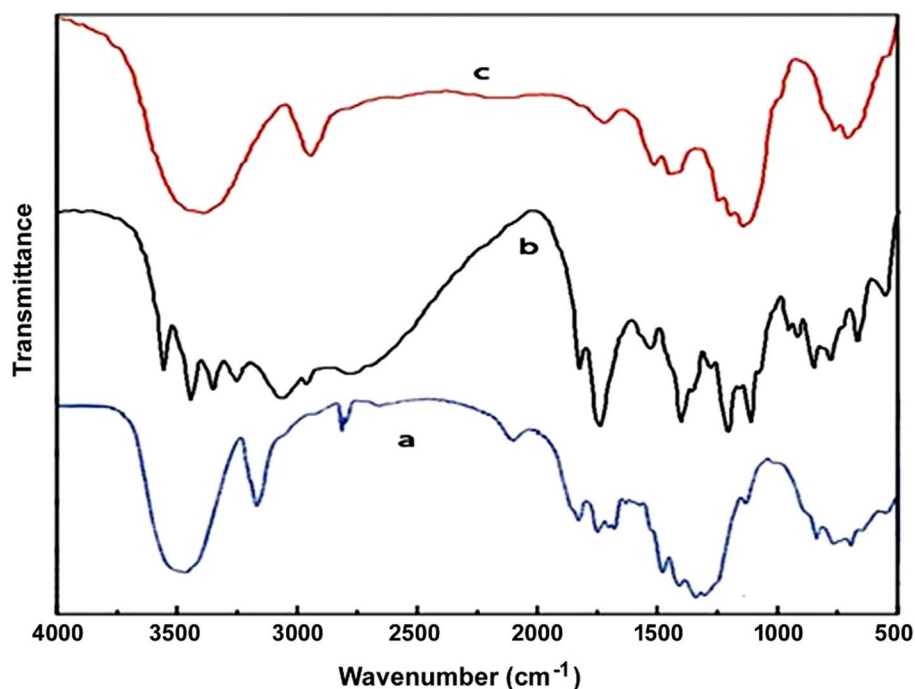
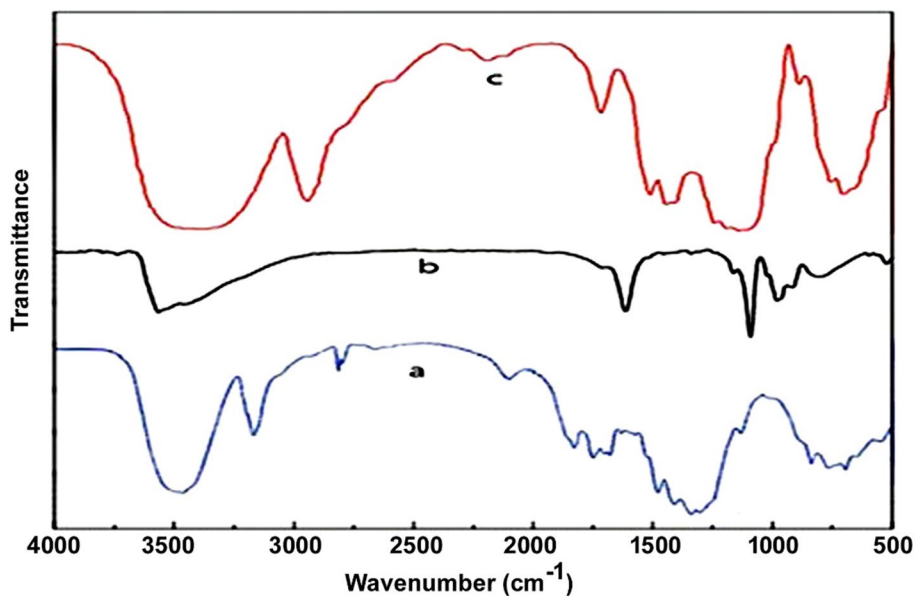


Fig. 9 FTIR spectra of (a) catenated nanocellulose, (b) ascorbic acid, and (c) catenated nanocellulose/ascorbic acid



from stretching C–O–C. Also C–O–C stretches are seen at 1142, 1121, 1113, and 1026 cm⁻¹. The peaks present in the region 990–1026 cm⁻¹ correspond to the lactone ring. The strong bands in the range 3216–3527 cm⁻¹ are assigned to the OH stretching due to the presence of moisture in the sample. Figure 9c shows that there are all vibrations related to chemical bonds in the cellulose and vitamin C. Compared with the CNPs structure (Fig. 9a) and AA (Fig. 9b), the bands arising from the synthesized CNPs/AA changed slightly either in intensity or in position.

These observations indicate to physical adsorption of AA on the CNPs caused some displacements in some bands. The composition of vitamin C comprises four hydroxyl groups with different acidities in positions 2, 3, 5, and 6 (Capuzzi et al. 1996). CNPs/AA complexes are proposed to be formed by non-covalent bonds, such as H bonds between the Preyssler's hydroxy group of vitamin C and W–O–W groups surrounding CNPs as a stabilizer in the solution.

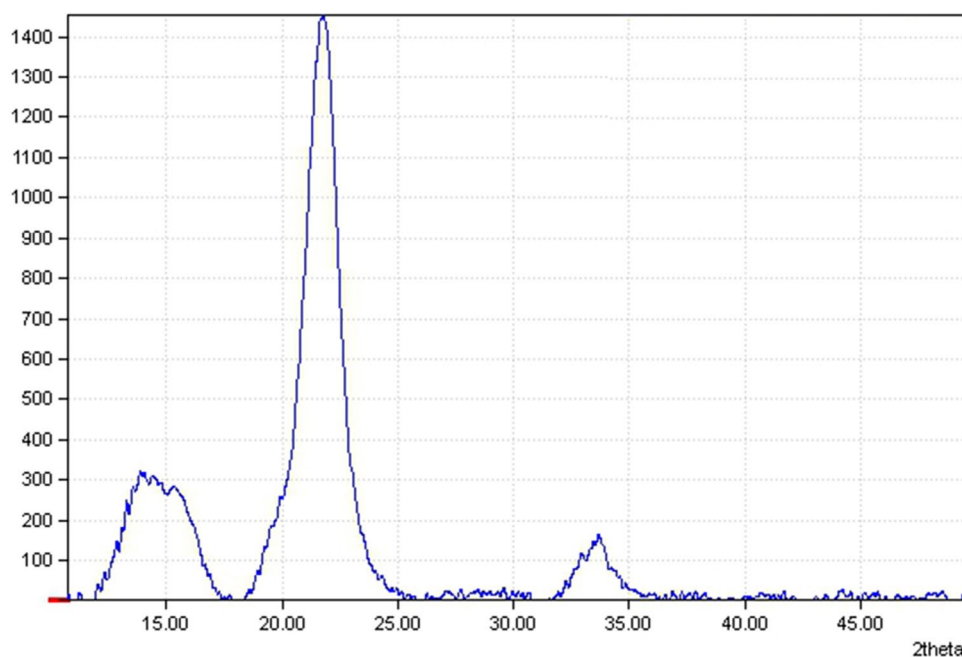
X-ray diffraction

Figure 10 presents the XRD patterns of synthesized nanocellulose. The XRD patterns of bare cellulose and preyssler heteropoly acid are shown in Figures S1 and S2 (supplementary information). The powder sample exhibits the well-known peaks of cellulose (Lefatshe et al. 2017). From XRD analysis, cellulose exhibited a monoclinic structure. The observed peaks at about $2\theta = 16^\circ$, 22° and 34° were attributed to the (101), (002) and (040) planes, respectively. These peaks correspond to cellulose I and were indexed to the database of ID number COD 4114994. X-ray patterns reveal the unresolved reflections of the (101), (002) and (040) planes, which indicates that the basic structure of bare cellulose was maintained in the CNPs. Powder XRD pattern of Preyssler sample showed diffraction peaks at $2\theta = 6.9^\circ$, 8.0° , 10.9° , 12.0° , 13.7° , 17.8° , 25.5° and 33.8° . The diffraction peaks of Preyssler sample is matched with the cubic structure of ammonium salt of Preyssler as reported in the literature (Al-Shehri and Katabathini 2018). This meant that none of the chemical or ultrasonic treatments altered the main structure according to the results of the FT-IR. Reducing the intensities of the reflections, possibly because of the presence of the preyssler around the CNPs.

SEM image

The CNPs/AA reported SEM image allows the AA to be seen distributed on the CNPs (Fig. 11). Following a non-oriented distribution, the entire surface is covered by the AA.

Fig. 10 X-ray patterns of the catenated nanocellulose



In vitro vitamin C releasing

We studied the release profiles of CNPs/AA at $37 \pm 0.5^\circ\text{C}$ to investigate the potential of using CNPs as a carrier for the controlled release of ascorbic acid. The combined profiles of AA release were analyzed with UV–vis spectroscopy and are shown in Fig. 12. As shown in Fig. 12, CNPs/AA is capable of controlling the AA release profile preventing an initial quick release. Fast release leads to higher initial drug delivery which in patients can cause some inconvenience. Besides, the rapid release reduces the carrier's effective service life (Huang and Brazel 2001). In general, during the 60 min the AA was released gradually, then during the 60–240 min (end of the experiment), the release rate was stable up. The number of AA published cumulatively was ca. 84.6%, within 1 h.

The release kinetics of AA in water at room temperature was also evaluated as $\ln C_A/C_{A0} = -kt$, where k is the rate constant and t is the release time (Table 1). The rate constant of first-order kinetics was calculated for five compositions of AA, by applying the regression function of Microsoft Excel 2010, obtaining best-fit results. The calculated r^2 values for all the equations were 0.99, indicating that the fitting application of the first-order kinetics is plausible. Our results indicate that the AA release kinetics depended on the composition of the mixture containing AA. Based on first-order kinetics, it can be stated that AA amount has an influence on the release rate. This behavior has been reported by different research groups (Khalid et al. 2013). Figure 13 shows that as the AA concentration increases, the amount of bounded AA to CNPs increases and the results in Table 1 suggest that with increasing the amount of bounded AA to CNPs, the rate

Fig. 11 SEM image of the catenated nanocellulose/ascorbic acid with different magnifications

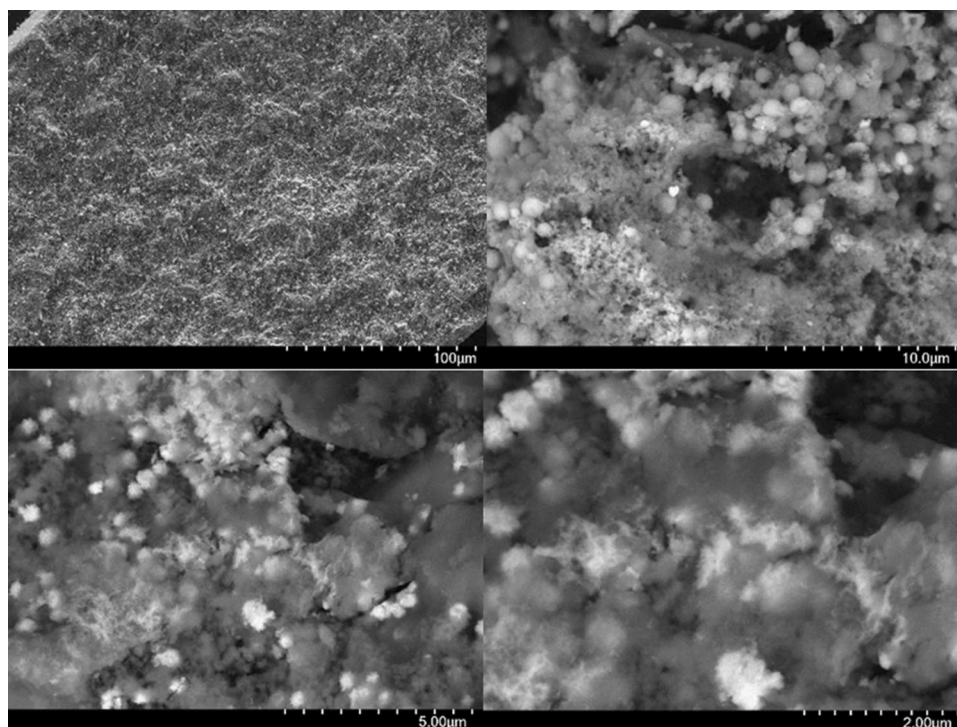


Fig. 12 UV–vis spectra for releasing of ascorbic acid as a function of time

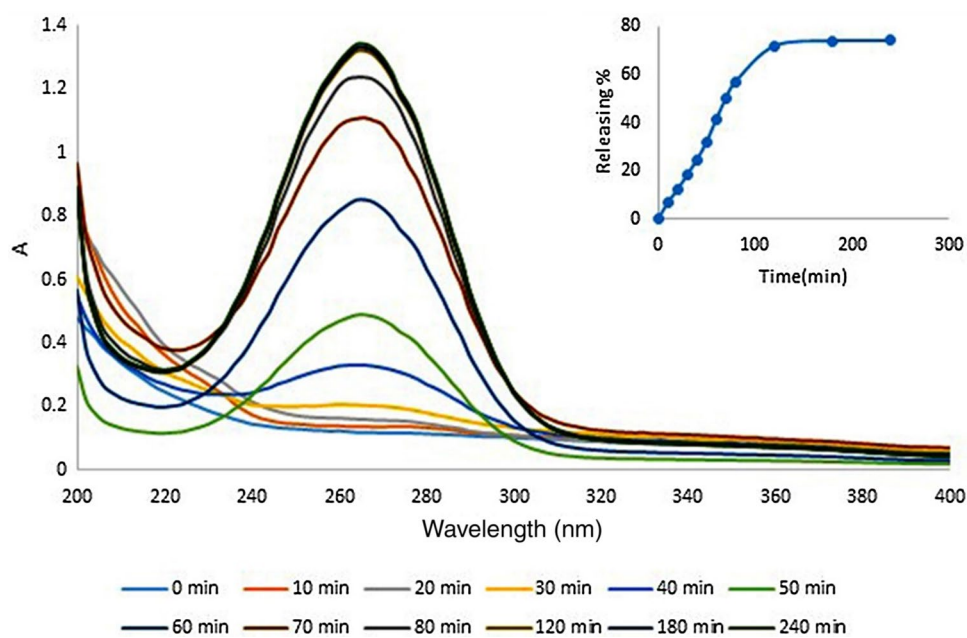
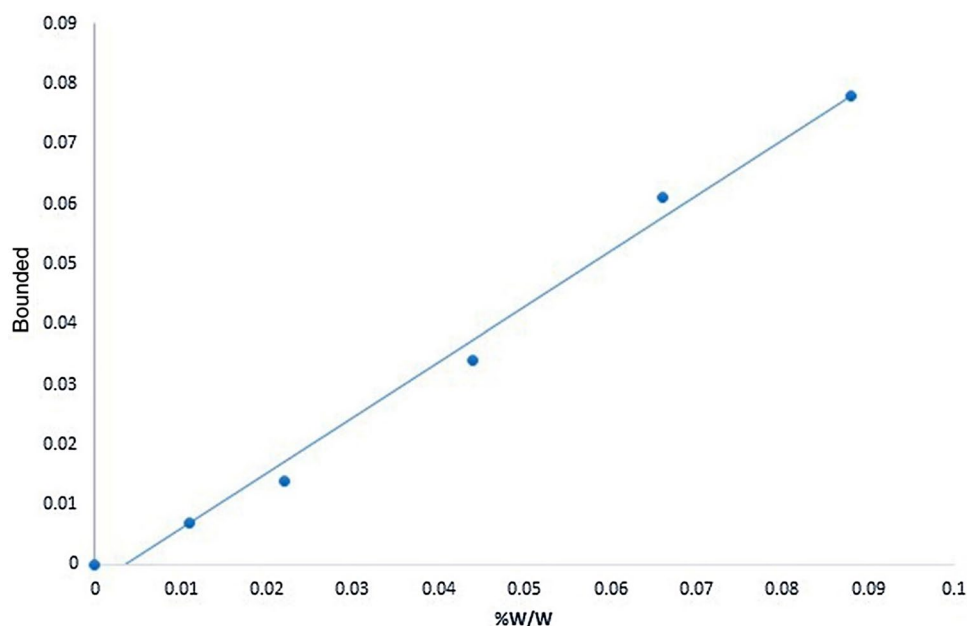


Table 1 Rate constants of AA release in various compositions of AA in CNPs/AA

AA concentration (%w)	Rate equation	Coefficient of determination (r^2)	Rate constant k
0.011	$\text{Ln}C_A/C_{A,0} = -0.006t$	0.99	0.006
0.022	$\text{Ln}C_A/C_{A,0} = -0.011t$	0.99	0.011
0.044	$\text{Ln}C_A/C_{A,0} = -0.014t$	0.99	0.014
0.066	$\text{Ln}C_A/C_{A,0} = -0.014t$	0.99	0.014
0.088	$\text{Ln}C_A/C_{A,0} = -0.012t$	0.99	0.012

Fig. 13 Effects of concentration of AA on the bounded amount of AA to CNPs



constant increases up to 0.044 w% and then becomes almost fixed. This observation is in accordance with the obtained data in Fig. 12. At first, the AA was released gradually, and after that, the release rate was stable up.

This means that the rate of AA releasing remains almost constant after the solution is saturated. The factors affecting the release kinetics of AA in different systems include the concentration of AA (active ingredient), the pH, and viscosity of the liquid phase and the preparation process, so this is a very complex process and its origin remains controversial.

Conclusion

In the presence of Preyssler acid, we infer from the above experimental results that catenated cellulose nanoparticles with high yield and reduced size have been successfully synthesized. The study is unique as we have shown that CNPs are formed using Preyssler as linker, stabilizer and interlocking agent through interfacial adhesion of cellulose nanoparticles via hydrogen bonds. X-ray patterns indicated that the basic structure of bare cellulose was maintained in the CNPs. Another element of this study emphasizes the potential of the synthesized CNPs as a nanocarrier and ascorbic acid releaser. Based on first-order kinetics, it can be concluded that AA amount have an influence on the release rate. The synthesis required aqueous phase in contrast to other approaches does not include harmful organic solvents and corrosive liquid acids and could, therefore, be known as green nanotechnology for drug and vitamin delivery applications.

Compliance with ethical standards

Conflict of interest The authors declare that they have no known competing financial interests or personal relationships that could have appeared to influence the work reported in this paper.

References

- Alizadeh MH, Harmalker SP, Jeannin Y et al (1985) A heteropolyanion with fivefold molecular symmetry that contains a nonlabile encapsulated sodium ion. The structure and chemistry of $[\text{NaP5W30O110}]^{14-}$. *J Am Chem Soc.* <https://doi.org/10.1021/ja00295a019>
- Al-Shehri A, Katabathini N (2018) Influence of polyoxometalate structure in ammoxidation of 2-methylpyrazine. *Catal Commun.* <https://doi.org/10.1016/j.catcom.2018.01.023>
- Ayati A, Ahmadpour A, Bamoharram FF et al (2014) Novel Au NPs/Preyssler acid/ TiO_2 nanocomposite for the photocatalytic removal of azo dye. *Sep Purif Technol* 133:415–420. <https://doi.org/10.1016/j.seppur.2014.06.055>
- Goudoulas T (2012) Polymers and biopolymers as drug delivery systems in nanomedicine. *Recent Pat Nanomed.* <https://doi.org/10.2174/1877913111202010052>
- Bamoharram FF, Heravi MM, Roshani M et al (2006) Preyssler catalyst, $[\text{NaP5W30O110}]^{14-}$: a green, efficient and reusable catalyst for esterification of salicylic acid with aliphatic and benzylic alcohols. *Appl Catal A Gen.* <https://doi.org/10.1016/j.apcata.2005.12.021>
- Bamoharram FF, Heravi MM, Saneinezhad S, Ayati A (2013) Synthesis of a nano organo-silicon compound for building materials waterproofing, using heteropolyacids as a green and eco-friendly catalyst. *Prog Org Coatings.* <https://doi.org/10.1016/j.porgcoat.2012.10.005>
- Bhatia S (2016) Chapter 2 nanoparticles types, classification, characterization, fabrication methods and drug delivery applications. *Natural polymer drug delivery systems.* https://www.springer.com/cda/content/document/cda_downloadaddocument/97833.19411:286-c1

- Börjesson M, Westman G (2015) Cellulose—fundamental aspects and current trends. Chapter 7. Crystalline nanocellulose—preparation, modification, and properties. InTech. doi: <https://doi.org/10.5772/61899>
- Capuzzi G, Lo Nostro P, Kulkarni K, Fernandez JE (1996) Mixtures of stearoyl-6-*O*-ascorbic acid and α -tocopherol: a monolayer study at the gas/water interface. *Langmuir*. <https://doi.org/10.1021/la960001y>
- Chamundeswari M, Jeslin J, Verma ML (2019) Nanocarriers for drug delivery applications. *Environ Chem Lett*
- Chaudhari A, Yan CCS, Lee SL (2005) Autopoisoning reactions over rough surface: a multifractal scaling analysis. *Int J Chem Kinet*. <https://doi.org/10.1002/kin.20062>
- Deepa B, Abraham E, Cherian BM et al (2011) Structure, morphology and thermal characteristics of banana nano fibers obtained by steam explosion. *Bioresour Technol*. <https://doi.org/10.1016/j.biortech.2010.09.030>
- Freeman R, Liu X, Willner I (2011) Chemiluminescent and chemiluminescence resonance energy transfer (CRET) detection of DNA, metal ions, and aptamer-substrate complexes using hemin/G-quadruplexes and CdSe/ZnS quantum dots. *J Am Chem Soc*. <https://doi.org/10.1021/ja202639m>
- Geibler D, Charbonniere LJ, Ziesel RF, Butlin NG, Lohmannsroben HG, Hildebrandt N (2010) Quantum dot biosensors for ultrasensitive multiplexed diagnostics. *Angew Chem Int Ed*. <https://doi.org/10.1002/anie.200906399>
- Gu X, Nguyen T, Oudina M et al (2005) Microstructure and morphology of amine-cured epoxy coatings before and after outdoor exposures—an AFM study. *J Coatings Technol Res*. <https://doi.org/10.1007/s11998-005-0014-x>
- Hallan SS, Kaur P, Kaur V, Mishra N, Vaidya B (2014) Lipid polymer hybrid as emerging tool in nanocarriers for oral drug delivery. *Artif Cells Nanomed Biotechnol*. <https://doi.org/10.3109/21691401.2014.95172>
- Hamid SBA, Al Amin M, Ali ME (2014) Zeolite supported ionic liquid catalyst for the synthesis of nanocellulose from palm tree biomass. *Adv Mat Res* 925:52–56
- Hamid SBA, Zain SK, Das R, Centi G (2016) Synergic effect of tungstophosphoric acid and sonication for rapid synthesis of crystalline nanocellulose. *Carbohydr Polym*. <https://doi.org/10.1016/j.carbpol.2015.10.023>
- Henriksson M, Henriksson G, Berglund LA, Lindström T (2007) An environmentally friendly method for enzyme-assisted preparation of microfibrillated cellulose (MFC) nanofibers. *Eur Polymer J* 43:3434–3441
- How CW, Rasedee A, Manickam S, Rosli R (2013) Tamoxifen-loaded nanostructured lipid carrier as a drug delivery system: characterization, stability assessment and cytotoxicity. *Colloids Surf B Biointerfaces*. <https://doi.org/10.1016/j.colsurfb.2013.08.009>
- Huang X, Brazel CS (2001) On the importance and mechanisms of burst release in matrix-controlled drug delivery systems. *J Contr Release* 73:121–136
- Jacob J, Haponiuk JT, Thomas S, Gopi S (2018) Biopolymer based nanomaterials in drug delivery systems: a review. *Mater Today Chem* 26:5533–5540
- Kaushik A, Singh M (2011) Isolation and characterization of cellulose nanofibrils from wheat straw using steam explosion coupled with high shear homogenization. *Carbohydr Res*. <https://doi.org/10.1016/j.carres.2010.10.020>
- Khadempir S, Ahmadpour A, Hamed Mosavian MT et al (2016) Mechanistic insights into the activation process in electrocatalytic ethanol oxidation by phosphomolybdic acid-stabilised palladium(0) nanoparticles (PdNPs@PMo12). *RSC Adv*. <https://doi.org/10.1039/c5ra22698h>
- Khalid N, Kobayashi I, Neves MA et al (2013) Preparation and characterization of water-in-oil-in-water emulsions containing a high concentration of L-ascorbic acid. *Biosci Biotechnol Biochem*. <https://doi.org/10.1271/bbb.120870>
- Kim DH, Kim KN, Kim KM, Lee YK (2008) Targeting to carcinoma cells with chitosan and starch coated magnetic nanoparticles for magnetic hyperthermia. *J Biomed Mater Res*. <https://doi.org/10.1002/jbm.a.31775>
- Kim JY, Kim SH, Rhee YS et al (2013) Preparation of hydroxypropylmethyl cellulose-based porous matrix for gastroretentive delivery of gabapentin using the freeze-drying method. *Cellulose*. <https://doi.org/10.1007/s10570-013-0048-7>
- Kingsley JD, Dou H, Morehead J, Rabinow B, Gendelman HE, Deschate CJ (2006) Nanotechnology: a focus on nanoparticles as a drug delivery system. *J Neuroimmune Pharmacol*. <https://doi.org/10.1007/s11481-006-9032-4>
- Klemm D, Kramer F, Moritz S et al (2011) Nanocelluloses: a new family of nature-based materials. *Angew Chemie Int Ed*. <https://doi.org/10.1002/anie.201001273>
- Kontturi E, Meriluoto A, Nuopponen M (2011) Process for preparing micro- and nanocrystalline cellulose. *Patents*
- Kozhevnikov IV (1987) Advances in catalysis by heteropolyacids. *Russ Chem Rev*. <https://doi.org/10.1070/rc1987v056n09abeh003304>
- Lee CK, Diesendruck CE, Lu E et al (2014) Solvent swelling activation of a mechanophore in a polymer network. *Macromolecules*. <https://doi.org/10.1021/ma500195h>
- Lee SL, Lee CK (1997) Heterogeneous reactions over fractal surfaces: a multifractal scaling analysis. *Int J Quantum Chem*. [https://doi.org/10.1002/\(SICI\)1097-461X\(1997\)64:3<337:AID-QUA6>3.0.CO;2-X](https://doi.org/10.1002/(SICI)1097-461X(1997)64:3<337:AID-QUA6>3.0.CO;2-X)
- Lefatshe K, Muiwa CM, Kebaabetswe LP (2017) Extraction of nanocellulose and in-situ casting of ZnO/cellulose nanocomposite with enhanced photocatalytic and antibacterial activity. *Carbohydr Polym*. <https://doi.org/10.1016/j.carbpol.2017.02.020>
- Levi-Polyachenko NH, Merkel EJ, Jones BT, Carroll DL, Stewart JH (2009) Rapid photothermal intracellular drug delivery using multiwalled carbon nanotubes. *Mol Pharm*. <https://doi.org/10.1021/mp800250e>
- Li X, Jiang Y, Wang L et al (2012) Effective low-temperature hydrolysis of cellulose catalyzed by concentrated H3PW12O40 under microwave irradiation. *RSC Adv*. <https://doi.org/10.1039/c2ra21022c>
- Liu Y, Wang H, Yu G et al (2014) A novel approach for the preparation of nanocrystalline cellulose by using phosphotungstic acid. *Carbohydr Polym*. <https://doi.org/10.1016/j.carbpol.2014.04.040>
- Loo C, Lowery A, Halas NJ, West J, Drezek R (2005) Immunotargeted nanoshells for integrated cancer imaging and therapy. *Nano Lett*. <https://doi.org/10.1021/nl050127s>
- Lopez-Davila V, Loizidou M (2012) Organic nanocarriers for drug delivery. *Curr Opin Pharmacol*. <https://doi.org/10.1016/j.coph.2012.02.011>
- Madani SY, Naderi N, Dissanayake O, Tan A, Seifalian AM (2011) A new era of cancer treatment: carbon nanotubes as drug delivery tools. *Int J Nanomed*. <https://doi.org/10.2147/IJN.S16923>
- Malam Y, Loizidou M, Seifalian AM (2009) Liposomes and nanoparticles: nanosized vehicles for drug delivery in cancer. *Trends Pharmacol Sci*. <https://doi.org/10.1016/j.tips.2009.08.004>
- Man Z, Muhammad N, Sarwono A, Bustam MA, Kumar MV et al (2011) Preparation of cellulose nanocrystals using an ionic liquid. *J Polym Environ* 19:726–731
- Mishra B, Patel BB, Tiwari S (2010) Colloidal nanocarriers: a review on formulation technology, types and applications toward targeted drug delivery. *Nanomedicine*. <https://doi.org/10.1016/j.nano.2009.04.008>
- Misono M (1987) Heterogeneous catalysis by heteropoly compounds of molybdenum and tungsten. *Catal Rev*. <https://doi.org/10.1080/01614948708078072>

- Muller RH (2000) Solid lipid nanoparticles (SLN) for controlled drug delivery—a review of the state of the art. *Eur J Pharm Biopharm* 49:211–218
- Okuhara T, Mizuno N, Misono M (1996) Catalytic chemistry of heteropoly compounds. *Adv Catal*. [https://doi.org/10.1016/S0360-0564\(08\)60041-3](https://doi.org/10.1016/S0360-0564(08)60041-3)
- Pathania D, Gupta D, Kothiyal NC, Eldesoky GE, Naushad M (2016) Preparation of a novel chitosan-g-poly (acrylamide)/Zn nanocomposite hydrogel and its applications for controlled drug delivery of ofloxacin. *Int J Biol Macromol* 84:340–348
- Purkait BS, Ray D, Sengupta S et al (2011) Isolation of cellulose nanoparticles from sesame husk. *Ind Eng Chem Res* 50:871–876
- Qian W, Sun D, Zhu R, Du X, Liu H, Wang S (2012) pH-sensitive strontium carbonate nanoparticles as new anticancer vehicles for controlled etoposide release. *Int J Nanomed*. <https://doi.org/10.2147/IJN.S34773>
- Saito T, Kimura S, Nishiyama Y, Isogai A (2007) Cellulose nanofibers prepared by TEMPO-mediated oxidation of native cellulose. *Biomacromol* 8:2485–2491
- Saneinezhad S, Bamoharram FF, Mozhdehi AM et al (2019) Functionalized cellulose-preyssler heteropolyacid bio-composite: an engineered and green matrix for selective, fast and in-situ preparation of Pd nanostructures: synthesis, characterization and application. *Arab Jour Che*. <https://doi.org/10.1016/j.arabjc.2019.10.006>
- Satyamurthy P, Jain P, Balasubramanya RH, Vigneshwaran N (2011) Preparation and characterization of cellulose nanowhiskers from cotton fibres by controlled microbial hydrolysis. *Carbohydr Polym*. <https://doi.org/10.1016/j.carbpol.2010.07.029>
- Shekh MI, Amirian J, Stadler FJ et al (2020) Oxidized chitosan modified electrospun scaffolds for controllable release of acyclovir. *Int J Biol Macromol*. <https://doi.org/10.1016/j.ijbiomac.2020.02.230>
- Singh A (2011) Biopolymers in drug delivery: a review. *Pharmacol online* 674:666–674
- Siqueira G, Tapin-Lingua S, Bras J, da Silva PD, Dufresne A (2010) Morphological investigation of nanoparticles obtained from combined mechanical shearing, and enzymatic and acid hydrolysis of sisal fibers. *Cellulose* 17:1147–1158
- Sun T, Zhang YS, Pang B, Hyun DC, Yang M, Xia Y (2014) Engineered nanoparticles for drug delivery in cancer therapy. *Angew Chem Int Ed*. <https://doi.org/10.1002/anie.201403036>
- Tian J, Wang J, Zhao S et al (2010) Hydrolysis of cellulose by the heteropoly acid H3PW12O40. *Cellulose*. <https://doi.org/10.1007/s10570-009-9391-0>
- Yavuz MS, Cheng Y, Chen J, Cogley CM, Zhang Q, Rycenga M, Xie J, Kim C, Song KH, Schwartz AG, Wang LV, Xia Y (2009) Gold nanocages covered by smart polymers for controlled release with near-infrared light. *Nat Mater*. <https://doi.org/10.1038/nmat2564>
- Yoo HS, Lee JE, Chung H, Kwon IC, Jeong SY (2005) Self-assembled nanoparticles containing hydrophobically modified glycol chitosan for gene delivery. *J Contr Release*. <https://doi.org/10.1016/j.jconrel.2004.11.033>
- Zhou YM, Fu SY, Zheng LM, Zhan HY (2012) Effect of nanocellulose isolation techniques on the formation of reinforced poly(vinyl alcohol) nanocomposite films. *Express Polym Lett*. <https://doi.org/10.3144/expresspolymlett.2012.85>
- Zhu JY, Sabo R, Luo X (2011) Integrated production of nano-fibrillated cellulose and cellulosic biofuel (ethanol) by enzymatic fractionation of wood fibers. *Green Chem*. <https://doi.org/10.1039/c1gc15103g>

Publisher's Note Springer Nature remains neutral with regard to jurisdictional claims in published maps and institutional affiliations.